Reduced Hydrophobicity of the Minor Groove Intercalation Loop is Critical for Efficient Catalysis by Cold Adapted Uracil-DNA N-Glycosylase from Atlantic Cod

Elin Moe[1]*, Netsanet Gizaw Assefa[1], Ingar Leiros[1], Kathrin Torseth[2], Arne O Smalås[1] and Nils Peder Willassen[1]

[1]*The Norwegian Structural Biology Centre, University of Tromsø, N-9037 Tromsø, Norway*

[2]*Department of Laboratory Medicine, Children's and Women's Health, Norwegian University of Science and Technology, N-7489 Trondheim, Norway*

Abstract

The minor groove intercalation loop (leucine-loop) in Uracil-DNA N-glycosylases (UNGs) undergoes significant conformational changes upon substrate interaction. Previous studies have shown that the cold adapted Atlantic cod UNG (cUNG) possesses a tenfold higher catalytic efficiency than human UNG (hUNG). A sequence alignment of the two enzymes revealed amino acid substitutions in and near the leucine-loop of cUNG which may increase the elasticity of the loop and thus explain the observed higher catalytic efficiency of cUNG compared to hUNG. In order to investigate this hypothesis we constructed five single and four multiple mutants of cUNG with cod to human UNG substitutions and characterised them by kinetic experiments at three different temperatures (15, 22 and 37°C) and Differential Scanning Calorimetry (DSC). The results showed that the mutations affected the k_{cat} more than the K_M, and mutants with apparent reduced hydrophobic properties (A266T, V267A, A266T/V267A and A266T/V267A/A274V) showed increased or equivalent k_{cat} to cUNG, while mutants with predicted increased hydrophobicity (A274V, H275Y, L279F, A266T/V267A/A274V/H275Y and A266T/V267A/A274V/H275Y/H250Q) showed reduced k_{cat} compared to cUNG. Thus, mimicking the amino acid composition of the leucine-loop in hUNG reduces the activity of cUNG. The DSC experiments were performed in order to identify a potential increase in the overall stability of the mutants as a result of altered hydrophobicity of the leucine-loop. However, the results showed a slight reduction in the overall stability for mutants with increased k_{cat} and increased stability for mutants with reduced k_{cat}. We suggest these results arise from a need to compensate for a potential increased/reduced elasticity of the leucine-loop which is introduced by the amino acid substitutions. This study confirms the suggested importance of the leucine-loop for efficient catalysis of UNG and shows that it is possible to alter the catalytic capacity of this enzyme by manipulating the amino acid composition of this loop.

Keywords: Cold adaptation of enzymes; DNA repair; Uracil-DNA N-glycosylase; Kinetics; Differential scanning calorimetry

Introduction

Uracil-DNA N-glycosylase (UNG) is a DNA repair enzyme involved in the base excision repair pathway (BER) for removal of uracil in DNA. Uracil in DNA may result from deamination of cytosine [1] or misincorporation during replication [2]. The crystal structure of the catalytic domain is known from a wide range of organisms including human [3], herpes simplex virus 1 (HSV-1) [4], *E. coli* [5], Atlantic cod [6], *D. radiodurans* [7], *Vibrio cholerae* [8], Vaccinia virus [9], *Mycobacterium tuberculosis* [10], *Bacillus substilis* (Banos-Sanz, 2013) and *Staphylococcus aureus* [11]. All ten enzymes have similar structures and consist of a classic single domain α/β-fold with a central four stranded parallel and twisted β-sheet surrounded by eight to eleven α-helices. The N- and C-terminals are on opposite sides of the central β-sheet and the active site is located within a positively charged groove at the C-terminal end of the parallel β-sheet.

The crystal structures have also been determined of UNG in complex with DNA from human [12-14], *Vaccinia virus* [15,16] and *D. radiodurans* [17]. These structures have revealed that the uracil is flipped out of the DNA and into the active site upon detection in a process where the enzyme binds the minor groove, compress the phosphate backbone and kink the DNA [13]. Three Ser-Pro-rich loops are involved in this process (named from the hUNG structure): the 4-Pro loop, the Gly-Ser loop and the minor groove intercalation loop (leucine loop). The four serines in these loops form hydrogen bonds to the phosphates 5' and 3' to uracil, and may orient the enzyme correctly for DNA scanning. The initial backbone compression is suggested to be coupled to a minor groove reading head formed by residues in the leucine loop which make water bridged hydrogen bonds to structurally conserved purine N3 sites and widens up the minor groove [13]. When the uracil is detected, it is flipped out of the DNA by further backbone compression, and the resulting DNA stabilised by penetration of a conserved Leucine (Leu272 in hUNG) into DNA minor groove [13]. It is further shown that the leucine plugging of the cavity in DNA increases the lifetime of the extrahelical base [18].

Cold adapted enzymes are characterised by low thermal stability and high catalytic efficiency compared to their mesophilic counterparts. It has been suggested that a consequence of the reduced stability is an increased flexibility which is necessary in order for the enzymes to perform efficient catalysis at low temperatures [19]. No general structural feature seems to account for the increased efficiency and reduced stability of the cold adapted enzymes [20]. However, for some enzymes correlations between cold adaptation and reduced interactions between structural domains or subunits are found. This is

observed for salmon trypsin [21], subtilisin from the Antarctic *Bacillus* TA39 [22], lactate dehydrogenase from Antarctic notothenoid fishes [23], citrate synthase from an Antarctic bacteria [24], phosphoglycerate kinase from Antarctic *Pseudomonas* sp. TACII18 [25], anionic trypsin from Chum salmon (*Oncorhynvhus keta*) [26] and alkaline phosphatase from Atlantic cod (*Gadus morhua*) [27]. These findings suggest local flexibility as a strategy for cold adaptation. Local flexibility is also suggested to be a strategy for cold adaptation of malate dehydrogenase from *Aquaspirillium arcticum* [28], chitobiase from *Arthrobacter* sp. TAD20 [29], DNA-ligase from *Pseudoalteromonas haloplanktis* [30] and alkaline proteinase from an Antarctic *Pseudomonas* species [31,32] argues that in order to increase the reaction rate of cold adapted enzymes, the best compromise would be to maximise the flexibility in the regions involved in catalysis and maintain or increase the rigidity in regions not involved in catalysis.

Cold adapted UNG has been isolated from the liver of Atlantic cod (*Gadus morhua*) and characterisation experiments revealed that it possesses cold adapted features, like increased catalytic efficiency and reduced temperature optimum for activity, compared to human UNG (hUNG) [33]. The catalytic domain of cod UNG (cUNG) has been produced (in *E. coli*) and purified, and characterisation experiments shows that the activity of cUNG is more thermolabile and has a 10-fold increase in catalytic efficiency at optimum conditions (pH 7.0 and 50 mM NaCl) compared to hUNG [34]. The crystal structure of the catalytic domain of cUNG has been determined at 1.9 Å resolution and a comparative analysis of the structures of cUNG and hUNG suggested that a less stable C-terminal part and an increased electrostatic surface potential near the active site might be responsible for the cold adapted behaviour of the cod enzyme [6]. The importance of an optimised positive electrostatic surface potential for the cold adapted features of cUNG has been confirmed experimentally by mutational and structural analysis [35], and theoretical calculation studies have suggested that cUNG in part uses local flexibility of the minor groove intercalation loop (leucine-loop) as a strategy for cold adaptation [6,36]. Recently the first thermal stability analysis of cUNG and hUNG, performed by DSC, was published and shows that the thermal melting temperature (T_m) of cUNG is 9°C lower than for hUNG [37]. Thus the overall stability of cUNG is lower than for hUNG and suggests that it is a more elastic molecule which is able to perform rapid conformational changes during catalysis at low temperatures. Lately the crystal structure and biophysical analysis of the complex of cUNG-Ugi (uracil DNA glycosylase inhibitor) further confirmed the importance of the optimised electrostatic surface potential for the high catalytic efficiency of cUNG compared to hUNG [38].

This study was initiated in order to investigate the hypothesis that a more dynamic leucine-loop of cUNG might contribute to the high catalytic efficiency of cUNG compared to hUNG in addition to the previously observed optimised electrostatic surface potential. Thus, nine mutants of cUNG were constructed, with cod to human UNG amino acid substitutions, and analysed by enzyme kinetics and DSC. In summary our results support the hypothesis that the high catalytic efficiency of the cold adapted UNG can in part be explained by a more dynamic leucine loop compared hUNG. However, the DSC experiments showed an unexpected reduced overall stability of the mutants with increased k_{cat} and increased overall stability for the mutants with reduced k_{cat}. We believe that this effect originates from a need to compensate for the increased/reduced rigidity which is introduced in the leucine-loop by the substitutions.

Materials and Methods

Materials

E. coli TOP10 [F - *mc*rA (*mrr-hs*dRMS-*mc*rBC) 8*0lac*Z M15 *lac*X74 *deo*R *rec*A1 *ar*aD139 (*ara-le*u) 7697 *gal*U *gal*K *rps*L (Str R) *end*A1 *nu*pG] was purchased from Invitrogen (Carlsbad, CA). *E. coli* NR8052 [Δ(*pro-lac, thi, ara, trpE9777, ung1*)], purified recombinant human UNG (UNGΔ84) and the gene encoding the catalytic domain of human UNG was kindly provided by Dr. Hans E. Krokan, Institute for Cancer Research and Molecular Biology, Norwegian University of Science and Technology.

Construction of mutants

The following mutants were constructed: A266T, V267A, Double (A266T/V267A), A274V, Triple1 (A266T/V267A/A274V), H275Y, Leuloop (A266T/V267A/A274V/H275Y), L279F and Triple2 (A274V, H275Y, L279F) The template for construction of the mutants was the gene encoding the catalytic domain of recombinant cod UNG with three additional codons (MEF) and two altered Arg codons (from AGA to CGT) in the N-terminal part of the sequence (cUNGΔ81) [34]. The Triple1, Leuloop and H275Y mutants were constructed as previously described [35]. The A266T, V267A, Double, A274V, L279F and Triple2 were constructed using the **QuickChange® Site-Directed Mutagenesis Kit** according to the manual from the manufacturer (Stratagene, CA). The primers used for the mutagenesis were as indicated in Table 1. The downstream primers are complementary and reverse of the primers listed in Table 1. The DNA sequencing was performed using BigDye® Terminator v3.1 Cycle Sequencing Kit (Applied Biosystems).

Expression

Large-scale expression was performed in 2 L baffled Erlenmeyer flasks using a Multitron Incubator shaker (Infors HT, Bottmingen, Switzerland). Fifty ml pre-cultures of *E. coli* NR8052 transformed with the *pTrc99A* plasmid containing genes encoding the mutants were used for inoculation of 0.5 L of LB-medium supplemented with 0.1% glucose and 100 μg/ml of ampicillin. The cells were grown at 37°C until OD$_{600}$

Mutant	5'-primer
A266T	CATGTCTTGCAA<u>ACC</u>GTTCATCCATCTC
V267A	CATGTCTTGCAAGCT<u>GCG</u>CATCCATCTCCTTTG
Double (A266T/V267A)	CATGTCTTGCAAACC<u>GCG</u>CATCCATCTCCTTTG
A274V	CCTTTGTCT<u>GTG</u>CATCGTGGGTTCCTTGGTTG
Triple1 (A266T/V267A/A274V)	GCAA<u>ACCGCG</u>CATCCATCTCCTTTGTCT<u>GTG</u>CATCGTG
H275Y	GTCTGCT<u>TAT</u>CGTGGGTTC
Leuloop (A266T/V267A/A274V/H275Y)	CTTGCAA<u>ACCGCG</u>CATCCATCTCCTTTGTCT<u>GTGTAT</u>CGTG
L279F	CCTTTGTCTGCTCATCGTGGGTTC<u>TTT</u>GGTTG
Triple2 (A274V/H275Y/L279F)	CCTTTGTCT<u>GTGTAT</u>CGTGGGTTC<u>TTT</u>GGTTG

Table 1: Primers used for construction of mutants.

was approximately 2.0. The expression was induced by adding IPTG to 1 mM concentration 30 minutes after lowering the temperature to 30°C or 20°C and the cells were harvested 5 hours or 16 hours after induction, respectively, by centrifugation.

Protein purification

The protein purification was performed using the Äkta Explorer Purification System (Amersham Biosciences, Uppsala, Sweden). Harvested cells from 4 L culture were re-suspended in 150 ml extraction buffer [25 mM Tris/HCl, 10 mM NaCl, 1 mM EDTA, 1% (v/v) glycerol, pH 8.0] and 4 Complete Mini EDTA-free Protease Inhibitor Cocktail tablets from Roche Applied Science (Indianapolis, USA) dissolved in 4 ml distilled water were added. The cells were disrupted on ice by ultrasonication using Sonics VC Ultrasonic Processor (Sonics & Materials, Inc., Newtown, USA) for one hour (9.9 seconds on, 9.9 seconds off) at 40% amplitude. The cell extract was centrifuged and the supernatant was collected. Thereafter, 2% (w/v) protamine sulfate was added to the final concentration of 0.25% (v/v) and incubated on ice for 15 min with stirring. The solution was centrifuged at 20,000 rpm for 1 hour at 4°C, and the supernatant was collected. The pH of the cell extract was adjusted to 7.5 followed by filtration using a 0.2 μm syringe filter (Millipore, Billerica, USA). The filtrate was then applied onto a Q-Sepharose FF column coupled with an SP Sepharose FF column, both equilibrated in 25 mM Tris/HCl, 10 mM NaCl, 1 mM EDTA, 1% (v/v) glycerol, pH 7.5]. The rest of the purification steps were performed as described above. Fractions containing UNG were pooled and concentrated using Amicon Centrifugal Filter Units (molecular weight cut off, 10 kDa) from Millipore.

Activity measurements

Nick translated calf thymus DNA (Sigma-Aldrich, Steinheim, Germany) with deoxy[5-^{3}H]uridine 5'-triphosphate (Amersham Biosciences, Uppsala, Sweden) was used as substrate. Preparation of substrate and measurement of UNG activity was performed as previously described [33]. The standard assay procedure is in short: The enzyme was diluted in cold dilution buffer (5 mM Tris-HCl, 10 mM NaCl, 1% glycerol, pH 8.0). The activity was measured in a total volume of 20 μl in 70 mM Tris-HCl, 10 mM NaCl, 1 mM EDTA, pH 8.0, 100 μg/ml BSA and 230 ng substrate (^{3}H-dUMP DNA). The reaction mixture was incubated for 10 minutes at 37°C, and terminated by addition of 20 μl ice cold single stranded calf thymus DNA (1 mg/ml) and 500 μl 10% TCA. After incubation on ice for 15 minutes, free ^{3}H uracil was separated from precipitated material by centrifugation at 16 000 g for 10 minutes, and analysed using a liquid scintillation counter. One unit enzyme is defined as the amount of enzyme required for release of 1 nmol acid soluble uracil per minute at 37°C.

Kinetics

K_M and k_{cat} were measured in the presence of eight different [^{3}H]-dUMP substrate concentrations in the range of 0.56 -4.5 μM at 15°C, 22°C and 37°C. The amounts of UNG used were different for each mutant at the different temperatures, giving cpm values between 500 - 5000. Assays were performed in 25 mM Tris-HCl, 50 mM NaCl, 1 mM EDTA and 100 μg/ml BSA, pH 7.5 at 37°C. The calculation of the kinetic constants was performed by the enzyme kinetics module in SigmaPlot (SPSS Inc., Chicago, IL).

Differential scanning calorimetry (DSC)

DSC experiments were conducted on a Nano-Differential Scanning Calorimeter III, model CSC6300 from Calorimetry Sciences

Corporation (Lindon, USA). Preparations of the native enzymes were dialyzed overnight at 4°C against 1 L of dialysis buffer [25 mm Hepes, 10 mM NaCl, 1 mM EDTA, 1% (v/v) glycerol, pH 7.4] in a Pierce Slide-A-Lyzer dialysis cassettes from Thermo Fisher Scientific Inc (Rockford, USA) with a 10 kDa cut-off followed by filtration using a 0.2 μm syringe filter (Millipore, Billerica, USA).

The dialysis buffers were used as reference buffers in the DSC runs. Reference buffers and samples were degassed for 10 minutes before loading into the DSC cells. The temperature scans were carried out at a constant pressure of 3 atm in a range 10 or 20 to 70°C with a heating or cooling rate of 1°C /min. Refolding experiments were performed for each protein by a backward cooling scan after unfolding and by incubating the unfolded proteins at 4°C for 1 hour before initiating a new forward scan. CpCalc software supplied with the instrument was utilized to generate molar heat capacity values. The experimental transition curves were fitted on a two-state transition model.

Results and Discussion

The minor groove intercalation loop (leucine-loop) undergoes significant conformational changes upon binding of UNG to substrate DNA and brings His268 within hydrogen binding distance of the uracil O$_2$, to accomplish the formation of the uracil recognition pocket. It also stabilises the distorted DNA when uracil is flipped into the specificity pocket [13,17,18] It is thus important that the loop consists of amino acids which allow rapid conformational changes upon interaction with DNA. A sequence alignment of cod and human UNG (Figure 1) revealed differences in the amino acid composition close to and within the leucine-loop which suggest improved dynamic properties of the cUNG loop.
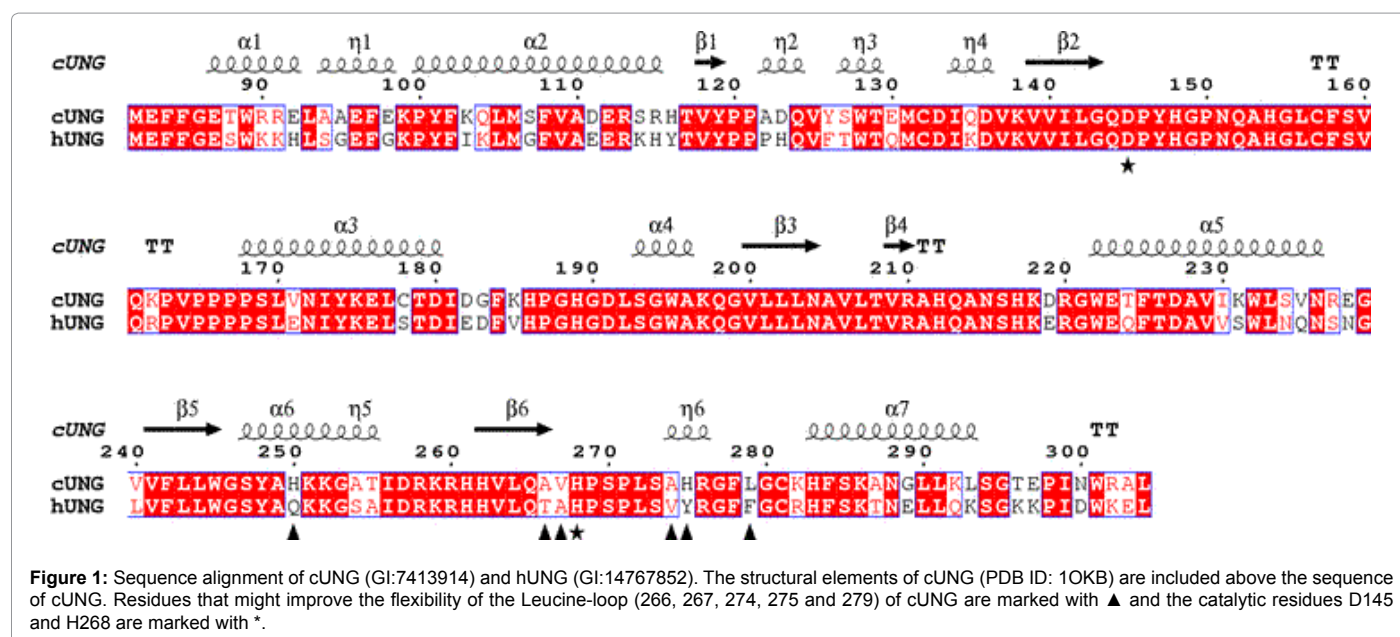
Two of the residues which anchor the leucine-loop to the β4 strand in hUNG, Thr266 and Ala267, is substituted by Ala and Val in cUNG. In addition are Val274, Tyr275 and Phe279 substituted by Ala, His and Leu in cUNG, respectively. Based on this observation, nine different mutants with both single and multiple substitutions were constructed and characterised with regard to catalytic efficiency and temperature stability (Tables 2 and 3). The positions of the substituted amino acids are shown in Figure 2.

The mutants were produced in large scale and purified following the procedures described earlier and diafiltrated. The yield varied, but was typically between 2-4 mg for each mutant. After purification, the kinetic constants, k_{cat} and K_M were determined for the mutants at 15°C, 22°C and 37°C using the optimal buffer conditions for cUNG (pH 7.5 and 50 mM NaCl). In addition, thermal stability was measured by DSC.

The A266T, V267A and A266T/V267A mutants shows similar and higher k_{cat} compared to cUNG

An analysis of the enzyme kinetics shows that the mutations affected the k_{cat} (turnover rate) more than the Michaelis-Menten constant (K_M), and in the case of the A266T mutant, the k_{cat} is similar to cUNG at all three temperatures and only slightly increased at 37°C. For the A267V mutant the k_{cat} value is similar to cUNG at 37°C, while it is reduced with approximately 50% at 22 and 15°C (Table 3). However, when these two mutations are combined in the A266T/V267A double mutant, the k_{cat} is increased with 40% compared to cUNG at 37°C, while it is slightly decreased with 14 and 2% compared to cUNG at 22 and 15°C, respectively (Table 3).

As mentioned above, A266 and V267 anchor the leucine-loop to the β4 strand in UNG and the substitutions to Thr and Ala, respectively,

Figure 1: Sequence alignment of cUNG (GI:7413914) and hUNG (GI:14767852). The structural elements of cUNG (PDB ID: 1OKB) are included above the sequence of cUNG. Residues that might improve the flexibility of the Leucine-loop (266, 267, 274, 275 and 279) of cUNG are marked with ▲ and the catalytic residues D145 and H268 are marked with *.

UNG	T (°C)	V_{max} (nmol/min/mg)		k_{cat} (min⁻¹)	K_M (µM)		k_{cat}/K_M (min⁻¹µM⁻¹)
cUNG [35]	37	49135	± 1626	1241	0.8	± 0.09	1499
	22	24439	± 555	617	0.8	± 0.06	795
	15	11064	± 374	279	0.5	± 0.07	607
A266T	37	53467	± 1079	1352	0.6	± 0.04	2282
	22	24994	± 464	632	1.0	± 0.05	641
	15	10006	± 170	253	0.7	± 0.04	389
V267A	37	47476	± 1363	1197	0.5	± 0.06	2507
	22	15218	± 313	384	0.6	± 0.04	685
	15	5867	± 113	148	0.3	± 0.03	500
Double (A266T/V267A)	37	68898	± 1455	1740	0.7	± 0.05	2500
	22	20891	± 320	528	0.8	± 0.04	686
	15	10805	± 249	273	0.5	± 0.05	549
A274V	37	37379	± 611	944	1.1	± 0.05	830
	22	11746	± 244	297	0.8	± 0.06	381
	15	8991	± 286	227	1.3	± 0.11	174
Triple1 (A266T/V267A/A274V)	37	61843	± 2879	1562	0.7	± 0.12	2199
	22	30544	± 733	771	0.8	± 0.07	929
	15	14550	± 509	367	0.7	± 0.09	496
H275Y [35]	37	23590	± 859	596	0.6	± 0.09	1017
	22	11974	± 553	302	0.6	± 0.11	509
	15	6166	± 384	156	0.7	± 0.16	224
Leuloop (A266T/V267A/A274V/H275Y)	37	26603	± 1293	672	0.7	± 0.12	1018
	22	10415	± 282	263	0.5	± 0.06	548
	15	6007	± 273	152	0.5	± 0.11	292
L279F	37	31674	± 321	800	0.5	± 0.02	1459
	22	11944	± 145	302	0.5	± 0.03	611
	15	7977	± 252	201	0.6	± 0.08	342
Triple2 (A274V/H275Y/L279F)	37	30569	± 676	713	0.8	± 0.06	919
	22	7551	± 160	176	0.8	± 0.05	215
	15	4352	± 79	102	0.7	± 0.04	146
hUNG [35]	37	25347	± 1256	647	2.1	± 0.23	309
	22	12530	± 740	320	2.4	± 0.29	135
	15	5580	± 399	142	2.2	± 0.34	66

Table 2: Kinetic constants of the interactions of cUNG and mutants with substitutions in the Leucine-loop with uracil (3H⁺ labelled) incorporated calf thymus DNA. The assay was performed at 15, 22 and 37°C in 25 mM Tris/HCl (pH 7.5 at 25°C), 50 mM NaCl, 1 mM EDTA. The V_{max} and K_m were extracted by fitting the velocity data obtained at 8 different substrate concentrations on the *Michaelis-Menten* equation using the enzyme kinetics module in Sigma Plot. The standard error (SD) for the fit is indicated.

UNG	37°C	22°C	15°C
cUNG	0	0	0
A266T	-9	-2	9
V267A	4	38	47
Double (A266T/V267A)	-40	14	2
A274V	24	52	19
Triple1 (A266T/V267A/A274V)	-26	-25	-32
H275Y	52	51	44
Leuloop (A266T/V267A/A274V/H275Y)	46	57	46
L279F	36	51	28
Triple2 (A274V/H275Y/L279F)	43	71	63
hUNG	48	48	49

Table 3: Reduction (%) in k_{cat} at different temperatures for cUNG mutants and hUNG relative to cUNG.
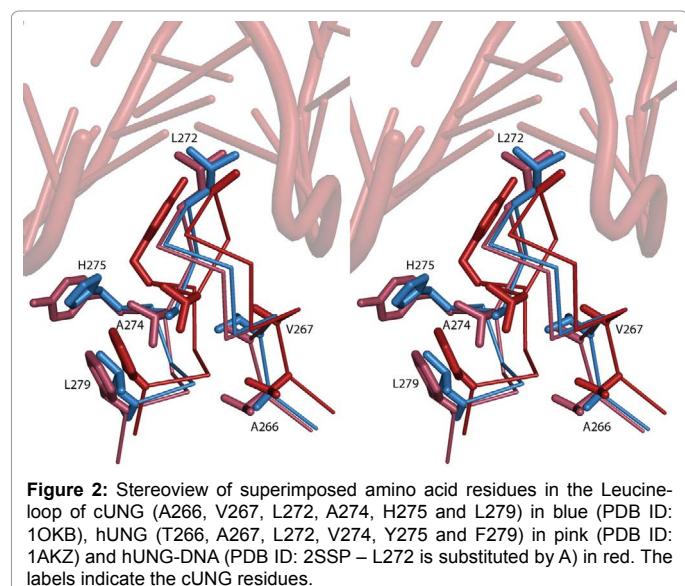

Figure 2: Stereoview of superimposed amino acid residues in the Leucine-loop of cUNG (A266, V267, L272, A274, H275 and L279) in blue (PDB ID: 1OKB), hUNG (T266, A267, L272, V274, Y275 and F279) in pink (PDB ID: 1AKZ) and hUNG-DNA (PDB ID: 2SSP – L272 is substituted by A) in red. The labels indicate the cUNG residues.

probably allow more elastic movements of the leucine-loop which give rise to a more efficient interaction with the damaged DNA. Why the k_{cat} is reduced by approximately 50% for the V267A mutant compared to cUNG at lower temperatures is difficult to explain. However, since electrostatic interactions are more strengthened at low temperatures, substituting the Valine with Alanine may affect one of the two observed hydrogen bonds between His268 and Gln144 or Leu272 and Arg276 in the leucine-loop in such a way that they get stronger, and thus reduces the dynamic properties of the loop and the k_{cat} at 22 and 15°C.

The H275Y substitution severely affects the k_{cat}

The k_{cat} of the V274A, H275Y and L279F mutants are strongly reduced compared to cUNG with most effect on the H275Y mutant which has an approximate reduction of 50% in k_{cat} at all temperatures (Table 3), and indicates that His275 is very important for the high catalytic efficiency of cUNG. This has previously been observed through theoretical calculation studies [36], where one of the experiments showed that the side chain of Arg276 is closer to DNA in a cUNG-DNA complex than in hUNG-DNA, which is caused by a hydrogen bond between His275 and the O´5 atom on the adenine base opposite of the uracil pulling the DNA strand closer to the enzyme. From the structure of cUNG, it does not seem like His275 is able to interact strongly with

DNA, since it is pointing out from the minor groove of DNA (Figure 2). However the crystal structure of hUNG in complex with DNA, shows that the side chain of Tyr275 has changed conformation upon binding of DNA, pointing into the minor groove of DNA (Figure 2), and even though the crystal structure of cUNG in complex with DNA has not been determined, we assume that the same will happen with His275. This movement was observed in the model made of cUNG in complex with DNA in the theoretical study [30].

Thus His275 in cUNG probably interacts more strongly with DNA compared to Tyr275 in hUNG, and explains why the catalytic efficiency is severely reduced for the H275Y mutant (Table 2). However, the H275Y mutant shows no significant difference in K_M compared to cUNG, rather the reduction in catalytic efficiency is caused by a reduction in k_{cat}. One explanation for this could be that the His275 residue binds stronger to the transition state than to the ground state, affecting k_{cat} instead of K_M [39]. A strong interaction between the leucine-loop in cUNG and DNA is supported by a mutational study of Arg276 in hUNG, which shows its importance for the activity of hUNG due to favourable interactions with DNA [40].

The multiple mutants confirm the importance of the H275Y substitution

When we combine the A274V, H275Y and L279F mutations in the A274V/H275Y/L279F mutant, the k_{cat} value is even more reduced than for the H275Y mutant at 22 and 15°C, showing an approximate reduction of k_{cat} of 70 and 60% compared with cUNG, respectively, while it is slightly higher than for the H275Y single mutant at 37°C (Tables 2 and 3). The main contributor to the reduced k_{cat} is obviously the H275Y mutation, however it seems like the two other mutations has additional effects. Looking into the structures of cUNG and hUNG again (Figure 2), it seems likely that Val274, Tyr275 and Phe279 generates a hydrophobic cluster in the leucine-loop which may rigidify the loop. The equivalent residues in cUNG are Ala274 and Leu279 in addition to His275 which probably allow more elastic movements of the loop and thus a more efficient interaction with DNA (Figure 2). The V274, Y275 and F279 in the A274V/H275Y/L279F mutant probably generate a similar hydrophobic cluster in the leucine-loop, thus making the loop more rigid and preventing it from rapid conformational changes upon binding to DNA. Results from a molecular dynamic (MD) simulation of cUNG supports this theory showing reduced dynamic properties of the leucine-loop in hUNG compared to cUNG [36]. The same study showed that substituting only His275 with Tyr results in a reduced flexibility of the leucine-loop compared to native cUNG.

The high k_{cat} of the A266T/V267A/A274V mutant is difficult to explain but might be caused by an increased elasticity which is allowed by the A266T and V267A. However, by adding the H275Y substitution in the A266T/V267A/A274V/H275Y mutant, the k_{cat} is reduced. As seen before, the H275Y single mutant has severe effect on k_{cat} of cUNG alone, and is probably causing the k_{cat} to drop also for this multiple mutant, due to less efficient interactions with the DNA.

The substitutions affect the stability of cUNG in an unexpected manner

In order to analyse whether the amino acid substitutions in the leucine-loop had any effect on the overall stability of the protein, T_m was determined of the mutants by DSC. For every experiment in the order of 1-2 mg of protein was used, and all the measurements were performed by increasing the temperature by 1°C every minute until the melting curve was completed. The reversibility of the unfolding

was tested by slowly cooling down the protein solution in the sample cell and re-running the DSC experiment, however we were not able to detect any new melting curves, thus the unfolding was irreversible. This was confirmed by visual inspections of the protein solutions after the experiment which showed white protein aggregates, and is in accordance with previous results from thermal stability analysis of cUNG and hUNG [37].

The results from the DSC experiments show that T_m was only slightly decreased or increased for the mutants compared to cUNG (Figure 3). The mutants with T_m lower than cUNG were A274V (43.4°C), H275Y (43.8°C), Triple2 (44.0°C), Leuloop (44.4°C) and Triple1 (44.6°C) while mutants with higher T_m were Double (45.3°C), A266T (46.1), L279F (46.5°C) and V267A (46.5°C) (Table 4). The differences in T_m between native cUNG and the mutants is not large, with only a 1.7 and 1.3°C reduction in T_m for the A274V and H275Y substitutions respectively and a 1.0 and 1.6°C increase for the A266T and V267A substitutions. Such subtle changes in T_m caused by mutations analyzed by DSC is a common phenomenon and have been reported for other cold adapted enzymes like α-amylase from *Pseudoalteromonas haloplanktis* (AHA) [41] and chitinase from the Antarctic *Arthrobacter Sp. TAD20* [42].

Our hypothesis for this experiment was that the substitutions introduced in the leucine-loop would alter the rigidity of the loop and increase or reduce the overall s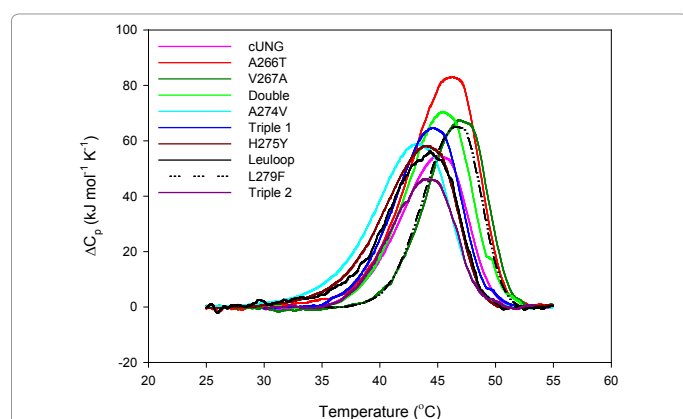tability accordingly. According to the hypothesis about an inverse relationship between activity and stability [23], we expected to observe reduced stability of the mutants with increased elasticity, and increased stability of the mutants with reduced elasticity. However, as observed from the results, this is not the case. Instead the mutants with increased hydrophobicity (A274V, H275Y, Triple1, Triple2 and Leuloop) possessed reduced stability, while mutants with reduced hydrophobicity (A266T, V267A, Double and L279F) possessed increased stability. Thus, the mutations affected the overall stability of the protein, however it seems like the changes can only be related to overall instead of local structural rearrangements which occur due to the substitutions and has to be evaluated separately from the changes in activity which are observed of the mutants.

Free energy (ΔG) of hydration explains unexpected stability results

The free energy (ΔG) of hydration is generally unfavourable for hydrophobic amino acids in contact with water at higher temperatures and destabilises proteins [43]. This effect is probably causing the reduced thermostability which is observed of the A274V, H275Y, Triple1, Triple2 and Leuloop mutants (Figure 3).

This theory also counts for the observed increased stability of the A266T, V267A and Double mutant, which probably is caused by the less unfavourable effect the reduced hydrophobicity has on the free energy (ΔG) of hydration.

Some of the activity measurements have been performed at 37°C, and as we can see from the DSC experiments (Figure 3), it seems like the unfolding process has started for both A274V and H275Y at temperatures below this temperature. Based on this result it is tempting to explain the reduced k_{cat} of these mutants with reduced overall stability at 37°C instead of an increased rigidity of the leucine-loop. However, the activity measurements are performed in the presence of DNA, which most likely increase the overall stability of the protein at the same time as it induce conformational changes of the loops and residues in the loops (e.g., Tyr275 in hUNG) which are involved in catalysis [12,13]. This is also well supported by results from a heat inactivation experiment we previously performed of the H275Y mutant, which showed an apparent increased stability of the H275Y mutant compared to cUNG upon substrate binding [35].

The ΔH_{cal} is increased for all the mutants compared to cUNG except Triple2, indicating that an increased amount of energy is needed to break the intramolecular interactions during the unfolding process of the proteins and thus an enhanced stability of the mutants. These results contradict the T_m values showing that several of the mutants possess reduced stability compared to cUNG. However, ΔH_{cal} is also a measure of energy which takes into consideration hydration effects upon unfolding in addition to bond breaking, and due to the aggregation of the protein we would thus be careful to draw any conclusion regarding the ΔH_{cal} of our mutants.

Stability/flexibility and activity relationships

The high catalytic activity of cold adapted enzymes is explained by an increased flexibility (and thus reduced stability) of the proteins which will allow rapid conformational changes at low temperatures [23]. There is growing evidence based on mutagenesis studies that increased catalytic activity of cold adapted enzymes is not always associated with reduced stability, and reduced stability is not always indicative of increased molecular flexibility [44]. Such delicate balance between activity and stability have been reported for subtilisin S41 from the Antarctic *Bacillus TA41* [45], chitinase from the Antarctic *Arthrobacter*

Figure 3: DSC unfolding curves of cUNG and nine cUNG mutants with amino acid substitutions in the Leucine-loop. The transition curves were obtained at 1°C/min scan rate in a buffer [25 mM Hepes, 10 mM NaCl, 1 mM EDTA, 1% (v/v) glycerol, pH 7.4]. The thermograms are baseline-subtracted and normalized for protein concentration.

UNG	ΔH_{Cal} (kJ/mol)	T_m (°C)
cUNG	351	45.1
A266T	564	46.1
V267A	406	46.7
Double (A266T/V267A)	489	45.3
A274V	443	43.4
Triple1 (A266T/V267A/A274V)	472	44.6
H275Y	460	43.8
Leuloop (A266T/V267A/A274V/H275Y)	448	44.4
L279F	420	46.5
Triple2 (A274V/H275Y/L279F)	350	44.0

Table 4: Thermodynamic stability parameters of native and mutant cUNG in Hepes buffer by DSC. The heating rate was 1°C per min. The experiments were performed at least twice, and resulted in reproducible T_m values irrespective of the protein concentration used. The molar heat capacity data extracted from experimentally obtained transition curves were deconvoluted on a two-state transition model using CpCalc software. The unfolding was irreversible.

Sp. TAD20 [42] and alkaline phosphatase (AP) from the Antarctic strain TAB5 [46]. This has also been demonstrated in our study which shows that variants with reduced k_{cat} compared to the wild type enzyme were not found to be more stable, and vice versa. A274V, H275Y, Leuloop, Triple1 and Triple2 were characterized by reduction of both enzymatic activity and stability while an improvement of both parameters was observed for A266T, V267A and Double. The only mutant which behaves according to the simple inverse relationship between activity and stability is the L279F mutant who possesses a 1°C increase in T_m and a 40% reduction in activity at 37°C compared to cUNG. Since we do not have the structure of this mutant, the explanation for this behaviour will only be speculative, but through its location at the edge of the leucine-loop (Figure 2) it might generate stabilising interaction with His275 in the loop making it less prone to hydration by surrounding water molecules, and increase the stability of the leucine-loop and thus the overall stability of the enzyme. The features of the Triple1 mutant are also different from the others by possessing both increased stability and activity. A similar result is observed for a mutant of subtilisin from the Antarctic bacillus TA39 [22] and reveals interesting options for industrial application of cold adapted enzymes.

Through theoretical calculation studies it has been suggested that the leucine-loop is more flexible in cUNG than in hUNG, which in combination with an optimized electrostatic surface potential, probably explains the increased catalytic efficiency of cUNG compared to hUNG [36]. We have through this study shown that an increased hydrophobicity of the leucine-loop reduces the activity of cUNG. However, the expected increased rigidity of the loop is not reflected in an increased overall stability, instead showed mutants with expected increased stability reduced stability and vice versa. This corresponds to the findings published by suggesting that a maximised flexibility in regions involved in catalysis in combination with an increased overall rigidity in other parts of the protein is a good compromise for increasing the reaction rate of cold adapted enzymes [32]. Thus, we propose that the increased hydrophobicity which has been introduced in the leucine-loop mutants resulted in an increased rigidity of the loop which has been compensated for by reducing the overall stability of the protein and vice versa.

Conclusion

The minor groove intercalation loop (leucine-loop) is very important for efficient removal of uracil in DNA by bringing the catalytic residue His268 within hydrogen binding distance of uracil, accomplishing the formation of the substrate binding pocket and stabilising distorted DNA when uracil is flipped into the specificity pocket [13,18]. Here, we have studied how substitutions of hydrophobic residues close to and in the leucine-loop affect the activity and overall stability of Atlantic cod UNG (cUNG). Based on our results we suggest that the reduced hydrophobicity of the leucine-loop in cUNG, increases its dynamic properties and thus optimizes the interaction between the leucine-loop and damaged DNA compared to hUNG. Our results confirm the importance of the leucine-loop for catalysis by UNG, and show how the capacity of this enzyme can be altered by manipulating the amino acid content of this loop.

Acknowledgements

References

1. Lindahl T, Nyberg B (1974) Heat-induced deamination of cytosine residues in deoxyribonucleic acid. Biochemistry 13: 3405-3410.

2. Tye BK, Nyman PO, Lehman IR, Hochhauser S, Weiss B, et al. (1977) Transient accumulation of Okazaki fragments as a result of uracil incorporation into nascent DNA. Proc Natl Acad Sci USA 74: 154-157.

3. Mol CD, Arvai AS, Slupphaug G, Kavli B, Alseth I, et al. (1995) Crystal structure and mutational analysis of human uracil-DNA glycosylase: structural basis for specificity and catalysis. Cell 80: 869-878.

4. Savva R, McAuley-Hecht K, Brown T, Pearl L (1995) The structural basis of specific base-excision repair by uracil-DNA glycosylase. Nature 373: 487-493.

5. Saikrishnan K, Bidya Sagar M, Ravishankar R, Roy S, Purnapatre K, et al. (2002) Domain closure and action of uracil DNA glycosylase (UDG): structures of new crystal forms containing the Escherichia coli enzyme and a comparative study of the known structures involving UDG. Acta Crystallogr D Biol Crystallogr 58: 1269-1276.

6. Leiros I, Moe E, Lanes O, Smalås AO, Willassen NP, et al. (2003) The structure of uracil-DNA glycosylase from Atlantic cod (Gadus morhua) reveals cold-adaptation features. Acta Crystallogr D Biol Crystallogr 59: 1357-1365.

7. Leiros I, Moe E, Smalås AO, McSweeney S (2005) Structure of the uracil-DNA N-glycosylase (UNG) from Deinococcus radiodurans. Acta Crystallogr D Biol Crystallogr 61: 1049-1056.

8. Raeder IL, Moe E, Willassen NP, Smalås AO, Leiros I (2010) Structure of uracil-DNA N-glycosylase (UNG) from Vibrio cholerae: mapping temperature adaptation through structural and mutational analysis. Acta Crystallogr Sect F Struct Biol Cryst Commun 66: 130-136.

9. Schormann N, Grigorian A, Samal A, Krishnan R, DeLucas L, et al. (2007) Crystal structure of vaccinia virus uracil-DNA glycosylase reveals dimeric assembly. BMC Struct Biol 7: 45.

10. Kaushal PS, Talawar RK, Varshney U, Vijayan M (2010) Structure of uracil-DNA glycosylase from Mycobacterium tuberculosis: insights into interactions with ligands. Acta Crystallogr Sect F Struct Biol Cryst Commun 66: 887-892.

11. Wang HC, Hsu KC, Yang JM, Wu ML, Ko TP, et al. (2014) Staphylococcus aureus protein SAUGI acts as a uracil-DNA glycosylase inhibitor. Nucleic Acids Res 42: 1354-1364.

12. Slupphaug G, Mol CD, Kavli B, Arvai AS, Krokan HE, et al. (1996) A nucleotide-flipping mechanism from the structure of human uracil-DNA glycosylase bound to DNA. Nature 384: 87-92.

13. Parikh SS, Mol CD, Slupphaug G, Bharati S, Krokan HE, et al. (1998) Base excision repair initiation revealed by crystal structures and binding kinetics of human uracil-DNA glycosylase with DNA. EMBO J 17: 5214-5226.

14. Parikh SS, Walcher G, Jones GD, Slupphaug G, Krokan HE, et al. (2000) Uracil-DNA glycosylase-DNA substrate and product structures: conformational strain promotes catalytic efficiency by coupled stereoelectronic effects. Proc Natl Acad Sci USA 97: 5083-5088.

15. Schormann N, Banerjee S, Ricciardi R, Chattopadhyay D (2015) Binding of undamaged double stranded DNA to vaccinia virus uracil-DNA Glycosylase. BMC Struct Biol 15: 10.

16. Burmeister WP, Tarbouriech N, Fender P, Contesto-Richefeu C, Peyrefitte CN, et al. (2015) Crystal Structure of the Vaccinia Virus Uracil-DNA Glycosylase in Complex with DNA. J Biol Chem 290: 17923-17934.

17. Pedersen HL, Johnson KA, McVey CE, Leiros I, Moe E, et al. (2015) Structure determination of uracil-DNA N-glycosylase from Deinococcus radiodurans in complex with DNA. Acta Crystallogr D Biol Crystallogr 71: 2137-2149.

18. Jiang YL, Kwon K, Stivers JT (2001) Turning On uracil-DNA glycosylase using a pyrene nucleotide switch. J Biol Chem 276: 42347-42354.

19. Hochachka PW, Somero GN (1984) Biochemical adaptation. Princeton University Press, Princeton, NJ, USA.

20. Smalås AO, Leiros HK, Os V, Willassen NP (2000) Cold adapted enzymes. Biotechnol Annu Rev 6: 1-57.

21. Smalås AO, Heimstad ES, Hordvik A, Willassen NP, Male R, et al. (1994) Cold adaption of enzymes: structural comparison between salmon and bovine trypsins. Proteins 20: 149-166.

22. Narinx E, Baise E, Gerday C (1997) Subtilisin from psychrophilic antarctic bacteria: characterization and site-directed mutagenesis of residues possibly involved in the adaptation to cold. Protein Eng 10: 1271-1279.

23. Fields PA, Somero GN (1998) Hot spots in cold adaptation: localized increases

in conformational flexibility in lactate dehydrogenase A4 orthologs of Antarctic notothenioid fishes. Proc Natl Acad Sci USA 95: 11476-11481.

24. Russell RJ, Gerike U, Danson MJ, Hough DW, Taylor GL, et al. (1998) Structural adaptations of the cold-active citrate synthase from an Antarctic bacterium. Structure 6: 351-361.

25. Bentahir M, Feller G, Aittaleb M, Lamotte-Brasseur J, Himri T, et al. (2000) Structural, kinetic, and calorimetric characterization of the cold-active phosphoglycerate kinase from the antarctic Pseudomonas sp. TACII18. J Biol Chem 275: 11147-11153.

26. Toyota E, Ng KK, Kuninaga S, Sekizaki H, Itoh K, et al. (2002) Crystal structure and nucleotide sequence of an anionic trypsin from chum salmon (Oncorhynchus keta) in comparison with Atlantic salmon (Salmo salar) and bovine trypsin. J Mol Biol 324: 391-397.

27. Asgeirsson B, Nielsen BN, Højrup P (2003) Amino acid sequence of the cold-active alkaline phosphatase from Atlantic cod (Gadus morhua). Comp Biochem Physiol B Biochem Mol Biol 136: 45-60.

28. Kim SY, Hwang KY, Kim SH, Sung HC, Han YS, et al. (1999) Structural basis for cold adaptation. Sequence, biochemical properties, and crystal structure of malate dehydrogenase from a psychrophile Aquaspirillium arcticum. J Biol Chem 274: 11761-11767.

29. Lonhienne T, Zoidakis J, Vorgias CE, Feller G, Gerday C, et al. (2001) Modular structure, local flexibility and cold-activity of a novel chitobiase from a psychrophilic Antarctic bacterium. J Mol Biol 310: 291-297.

30. Georlette D, Damien B, Blaise V, Depiereux E, Uversky VN, et al. (2003) Structural and functional adaptations to extreme temperatures in psychrophilic, mesophilic, and thermophilic DNA ligases. J Biol Chem 278: 37015-37023.

31. Aghajari N, Van Petegem F, Villeret V, Chessa JP, Gerday C, et al. (2003) Crystal structures of a psychrophilic metalloprotease reveal new insights into catalysis by cold-adapted proteases. Proteins 50: 636-647.

32. Lonhienne T, Gerday C, Feller G (2000) Psychrophilic enzymes: revisiting the thermodynamic parameters of activation may explain local flexibility. Biochim Biophys Acta 1543: 1-10.

33. Lanes O, Guddal PH, Gjellesvik DR, Willassen NP (2000) Purification and characterization of a cold-adapted uracil-DNA glycosylase from Atlantic cod (Gadus morhua). Comp Biochem Physiol B Biochem Mol Biol 127: 399-410.

34. Lanes O, Leiros I, Smalås AO, Willassen NP (2002) Identification, cloning, and expression of uracil-DNA glycosylase from Atlantic cod (Gadus morhua): characterization and homology modeling of the cold-active catalytic domain.

Extremophiles 6: 73-86.

35. Moe E, Leiros I, Riise EK, Olufsen M, Lanes O, et al. (2004) Optimisation of the surface electrostatics as a strategy for cold adaptation of uracil-DNA N-glycosylase (UNG) from Atlantic cod (Gadus morhua). J Mol Biol 343: 1221-1230.

36. Olufsen M, Smalås AO, Moe E, Brandsdal BO (2005) Increased flexibility as a strategy for cold adaptation: a comparative molecular dynamics study of cold- and warm-active uracil DNA glycosylase. J Biol Chem 280: 18042-18048.

37. Assefa NG, Niiranen L, Willassen NP, Smalås A, Moe E (2012) Thermal unfolding studies of cold adapted uracil-DNA N-glycosylase (UNG) from Atlantic cod (Gadus morhua). A comparative study with human UNG. Comp Biochem Physiol B Biochem Mol Biol 161: 60-68.

38. Assefa NG, Niiranen L, Johnson KA, Leiros HK, Smalås AO, et al. (2014) Structural and biophysical analysis of interactions between cod and human uracil-DNA N-glycosylase (UNG) and UNG inhibitor (Ugi). Acta Crystallogr D Biol Crystallogr 70: 2093-2100.

39. Olufsen M, Smalås AO, Brandsdal BO (2008) Electrostatic interactions play an essential role in DNA repair and cold-adaptation of uracil DNA glycosylase. J Mol Model 14: 201-213.

40. Chen CY, Mosbaugh DW, Bennett SE (2004) Mutational analysis of arginine 276 in the leucine-loop of human uracil-DNA glycosylase. J Biol Chem 279: 48177-48188.

41. D'Amico S, Gerday C, Feller G (2001) Structural determinants of cold adaptation and stability in a large protein. J Biol Chem 276: 25791-25796.

42. Mavromatis K, Feller G, Kokkinidis M, Bouriotis V (2003) Cold adaptation of a psychrophilic chitinase: a mutagenesis study. Protein Eng 16: 497-503.

43. Murphy KP (2001) Stabilization of protein structure. Methods Mol Biol 168: 1-16.

44. Huston AL, Haeggström JZ, Feller G (2008) Cold adaptation of enzymes: structural, kinetic and microcalorimetric characterizations of an aminopeptidase from the Arctic psychrophile Colwellia psychrerythraea and of human leukotriene A(4) hydrolase. Biochim Biophys Acta 1784: 1865-1872.

45. Miyazaki K, Wintrode PL, Grayling RA, Rubingh DN, Arnold FH (2000) Directed evolution study of temperature adaptation in a psychrophilic enzyme. J Mol Biol 297: 1015-1026.

46. Koutsioulis D, Wang E, Tzanodaskalaki M, Nikiforaki D, Deli A, et al. (2008) Directed evolution on the cold adapted properties of TAB5 alkaline phosphatase. Protein Eng Des Sel 21: 319-327.